PHYSICAL REVIEW B VOLUME 47, NUMBER 19 15 MAY 1993-I

Structural and electronic properties of GaP-AlP (001) superlattices

C. H. Park and K. J. Chang
Department of Physics, Korea Advanced Institute of Science and Technology, 373-1 Kusung-dong, Yusung-ku, Daejon, Korea
(Received 23 November 1992)

We present the results of *ab initio* pseudopotential calculations for studying the structural stability and the electronic structure of short-period $(GaP)_m(AlP)_m$ superlattices with m ranging from 1 to 6, composed of lattice-matched indirect-gap semiconductors. Both the bulk and epitaxial superlattices ordered in the CuAu-I, CuPt, and chalcopyrite structures are found to be unstable against phase segregation into their binary constituents at $T=0$. The bulk formation enthalpies are found to be similar to those for epitaxial superlattices grown on (001) GaP. The band gap of superlattices tends to decrease as the superlattice period increases. The ultrathin (001) superlattices with the superlattice period of $m=1$ and 2 show indirect-gap behavior while the direct band gap occurs for $m \geq 3$. Details of the electronic structure of superlattices are discussed based on the band-pushing and charge-confinement effects. The oscillator strength of the optical transition from the valence-band maximum to the conduction-band minimum state at the Γ point is found to be much stronger for even numbers of m. Both the monolayer and bilayer superlattices can be direct-gap semiconductors if substrates are selectively chosen with lattice constants above 5.48 and 5.47 Å, respectively.

I. INTRODUCTION

There has been a great deal of interest in direct-gap superlattices because of the potential applications for optoelectronic devices. With the development of epitaxial technology such as molecular-beam epitaxy or metal-organic chemical vapor deposition, it is possible to control the band structure of superlattices by varying the superlattice period and the substrate lattice constant. A periodic superlattice composed of two indirect-gap semiconductors provides the folding of the conduction-band minimum state into the zone-center position of the Brillouin zone.[1] With the combination of the pushing of electronic states[2,3] and the energy splitting due to substrate strain,[4] one can fabricate direct-gap superlattices from indirect-gap binary constituents. The Si-Ge system has been studied extensively in this category,[5] however, there is an intrinsic strain problem which results from a large lattice mismatch of 4% between Si and Ge. Thus the formation of defects at interfaces is inevitable during crystal growth.

On the other hand, among group III-V superlattices, GaP and AlP are nearly lattice matched with a small lattice mismatch of 0.2%. Since these materials are indirect with the conduction-band minimum state at the X point, the GaP-AlP (001) superlattices are considered as a realistic system for investigating the pseudodirect gap of superlattices. Several theoretical calculations have been reported to study the electronic structure and the optical properties of the GaP-AlP system.[6-8] Kim and Madhukar examined the electronic structure of GaP-AlP superlattices based on the usual sp^3 tight-binding method[6] and suggested that the (001) superlattice is direct. However, their calculational method is known to be a simple and convenient method of describing successfully only the valence-band structures. Kumagai and his co-workers used the sp^3s^* tight-binding method[7] which is capable of yielding more accurate conduction-band structures and found that the electronic structure and the optical transition are very sensitive to the band discontinuity and the optical oscillator strength is larger for shorter-period superlattices. Since these two calculations are based on the empirical approach and are not capable of predicting the accurate band discontinuity, they need some experimental knowledge on the band discontinuity, which is often used as a parameter when experimental data are not available. Schuurmans, Rompa, and Eppenga found an enhancement of the oscillator strength for the optical transition using the augmented spherical wave method and suggested the possibility of green light emission in monolayer superlattices.[8] Experimentally, short-period superlattices of $(GaP)_m(AlP)_m$ where m ranges from 4 to 10, grown by metal-organic vapor phase epitaxy, exhibited the emission peaks in photoluminescence.[9] These peaks shift toward higher energies and tend to increase in intensity as m decreases. These experimental results indicated that the $(GaP)_m(AlP)_m$ system is a type-II superlattice.

In this paper we study the structural and electronic properties of $(GaP)_m(AlP)_m$ superlattices using the first-principles pseudopotential method.[10] The thermodynamic stability of the CuAu-I-like, CuPt-like, and chalcopyritelike ordered structures[11] is examined. Because of the good lattice match between GaP and AlP, the formation enthalpies of bulk superlattices are found to be similar to those for epitaxial ones. However, both the bulk and epitaxial formations are found to be unstable against phase segregation into binary constituents at $T=0$. The $(GaP)_m(AlP)_m$ system is found to form the superlattices of a type-II band alignment and be pseudodirect-gap semiconductors for $m \geq 3$. For ultrathin superlattices with $m=1$ and 2, the level repulsion of electronic states,[2,3] which results from charge transfer at interfaces, is significant. The direct gaps found in superlattices with

$m \geq 3$ are found to be closely related to the confinement of conduction electrons into the AlP quantum wells. Compared with the unfolded state, such charge confinement is more significant for the folded state from the conduction-band minimum of indirect-gap constituents to the center of the superlattice Brillouin zone. The oscillator strength for optical transition is found to be stronger for even numbers of m. We also examine the effect of substrate strain on the energy band structure of the $(GaP)_m(AlP)_m$ system. Considering various substrates, we find that an indirect-to-direct gap transition is induced by enhancing the substrate lattice constant.

In Sec. II we describe the method of calculation. In Sec. III the structural stability of ordered bulk and epitaxial superlattices is discussed. The results of the calculations for the energy band structure and the oscillator strength for optical transition are presented and compared with other theoretical and experimental results. Discussions are also made. We summarize the results in Sec. IV.

II. CALCULATIONAL METHOD

In the calculations we use the self-consistent total-energy pseudopotential method[10] within the local-density-functional approximation.[12] The Ceperly-Alder correlation as parametrized by Perdew and Zunger is used.[13] Norm-conserving nonlocal pseudopotentials are generated by the scheme proposed by Hamann, Schlüter, and Chiang.[14] Semirelativistic corrections are included to ionic pseudopotentials.[15] The wave functions are expanded in a plane-wave basis set with a kinetic-energy cutoff of up to 12 Ry. To study the structural stability of superlattices, the summation of the charge density over the irreducible Brillouin zone (BZ) is performed using a set of $\mathbf{k}$ points for superlattices, which are equivalent to Chadi's ten special $\mathbf{k}$ points in the zinc-blende structure.[16,17] Thus this choice of equivalent sets of $\mathbf{k}$ points ensures consistency in the comparison of the total energies between the ordered superlattices and the pure binary compounds. The total energy is minimized by varying the lattice volume for bulk superlattices and the lattice constant perpendicular to a substrate for coherent epitaxial forms. Internal atomic positions are relaxed by calculating the Hellmann-Feynman forces[18] until the optimum atomic configuration is determined. To examine the electronic structure of thicker superlattices, we use the structural parameters which are determined by the valence force field model.[19]

III. RESULTS

A. Structural stability

The stability of a bulk superlattice in phase α with respect to phase segregation into binary constituents is determined by the enthalpy of formation $\Delta H^{(\alpha)}$ per anion-cation pair at $T=0$, defined as[20]

$$\Delta H^{(\alpha)}_{\text{bulk}}(Ga_{0.5}Al_{0.5}P) = E^{(\alpha)}(Ga_{0.5}Al_{0.5}P) - [E^{(\alpha)}(GaP) + E^{(\alpha)}(AlP)]/2 \ . \quad (1)$$

Here, $E^{(\alpha)}(Ga_{0.5}Al_{0.5}P)$, $E^{(\alpha)}(GaP)$, and $E^{(\alpha)}(AlP)$ are the enthalpies for $Ga_{0.5}Al_{0.5}P$, GaP, and AlP, respectively, in their equilibrium bulk structures. We consider three types of ordered structure to examine the stability of superlattices.[11,21,22] The CuAu-I- and CuPt-like structures with the alternating GaP and AlP monolayers have a long-range order along the [001] and [111] directions, respectively, while the two-layer $(GaP)_2/(AlP)_2$ superlattice is ordered along the [201] direction in the chalcopyrite-like structure.[11,21] Our calculated enthalpies of formation are given in Table I for both the bulk and epitaxial superlattices in the CuAu-I-like, CuPt-like, and chalcopyritelike structures. Similar enthalpy of formation of about 4 meV/atom is found for each ordered structure. Thus all the ordered structures of $Ga_{0.5}Al_{0.5}P$ alloys are unstable against phase segregation into binary constituents at $T=0$.

For systems of lattice-mismatched constituents, e.g., InP-GaP systems, it is generally known that the instability of superlattices is mainly originated from the excess elastic energy which is introduced to form the strained superlattice rather than the charge transfer between the different cation-anion bonds at the interface.[11,21,22] However, since the GaP-AlP superlattice is a good lattice-matched system, the elastic energy is significantly reduced compared with lattice-mismatched superlattices and the relaxation energy is almost negligible as shown in Table I. We find the energy increase result from the charge transfer between the Ga-P and Al-P bonds to be the main source of the instability. In other lattice-matched systems like AlAs-GaAs superlattices, similar behavior was also demonstrated.[11] For coherent epitaxial superlattices, a pseudomorphic strained lattice is grown on a substrate with the lattice constant parallel to the substrate restricted to that of the substrate. Since the GaP-AlP superlattices are well lattice matched to the GaP substrate considered here, the epitaxial formation enthalpies are almost identical to within 0.1 meV/atom to those for the bulk superlattices as shown in Table I.

B. Band offset

Our calculations of the band lineups at the GaP-AlP heterojunctions are performed by constructing the $(GaP)_4(AlP)_4$ superlattice, which consists of two slabs of

TABLE I. Calculated lattice constants (a_0 in units of Å), bulk (ΔH_{bulk}) and epitaxial (ΔH_{epi}) formation enthalpies (in units of meV/atom) are given for $Ga_{0.5}Al_{0.5}P$ alloys ordered in the CuAu-I-like, CuPt-like, and chalcopyritelike structures. The decomposition of the bulk formation enthalpies is given by the volume deformation (ΔE^v), charge transfer (ΔE^{ct}), and relaxation energies (ΔE^r).

	CuAu-I	CuPt	Chalcopyrite
a_0	5.366	5.363	5.363
ΔE^v	1.2	1.9	1.9
ΔE^{ct}	2.9	2.5	1.8
ΔE^r	−0.1	−0.1	−0.1
ΔH_{bulk}	4.0	4.3	3.6
ΔH_{epi}	3.9	4.2	3.6

the respective semiconductors in the [001] direction.[23] This supercell contains 16 atoms and two interfaces. Self-consistent solutions are obtained for both the charge density and the total potential, which is made of ionic, Hartree, and exchange-correlation potentials. The total potential for the angular momentum $l=1$ part of the nonlocal pseudopotentials is averaged in the plane parallel to the interface and plotted along the [001] superlattice direction in Fig. 1. Here, the $l=1$ pseudopotential is taken as local potential because it is important in determining the lineup of the p-like valence-band maximum.[23] We find the interface potential to be bulklike in the intermediate regions between the interfaces and confirm that two interfaces are sufficiently separated. The potentials marked by $\overline{V}_{\mathrm{AlP}}$ and $\overline{V}_{\mathrm{GaP}}$ in Fig. 1 correspond to the average levels in their bulk regions and are found to be -0.11 and 0.11 eV, respectively. Thus the difference between the two average levels, $\Delta\overline{V}=\overline{V}_{\mathrm{GaP}}-\overline{V}_{\mathrm{AlP}}$, is estimated to be 0.22 eV. We find that the valence-band maxima in bulk GaP and AlP are 10.02 and 9.74 eV, respectively, with respect to the corresponding average level of potential. After lining up the energy levels as shown in Fig. 2, a discontinuity of the valence band is estimated to be $\Delta E_v=0.49$ eV, with an upward step in going from AlP to GaP. Although the spin-orbit splittings are included *a posteriori*, the valence-band discontinuity is found to be little affected and a value of $\Delta E_v=0.50$ eV is obtained with the use of the measured spin-orbit splittings[24] of 0.08 and 0.04 eV for GaP and AlP, respectively. Our result for ΔE_v is in good agreement with one empirical value of 0.46 eV suggested by Tersoff[25] whereas it is larger than the previous pseudopotential calculation of 0.36 eV.[23] The difference between the present and previous *ab initio* calculations seems to result from the use of different parameters in calculations; a smaller kinetic-energy cutoff of 6 Ry and the calculated equilibrium volume were used in the previous work while we use the measured equilibrium volume.

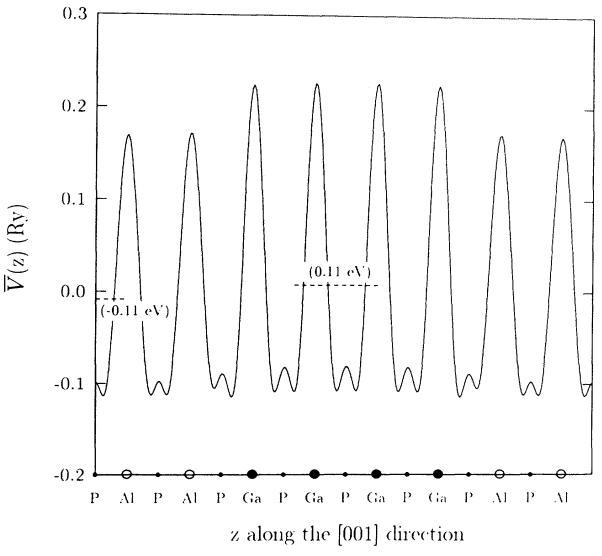

FIG. 1. Planar averaged $l=1$ component of the total potential $\overline{V}(z)$ in the GaP-AlP system. The average levels of two bulk potentials are represented by the dashed lines.

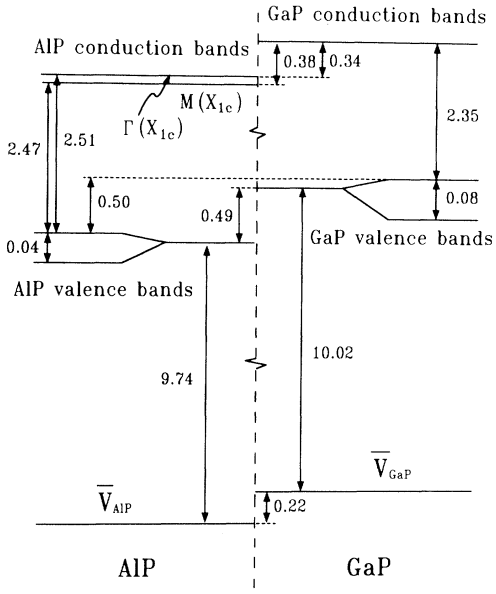

FIG. 2. Band lineups are drawn with the energies positioned relative to the average potentials $\overline{V}_{\mathrm{GaP}}$ and $\overline{V}_{\mathrm{AlP}}$. Energies are in units of eV. The spin-orbit splittings are given and the band splitting of the AlP conduction bands results from strain.

In determining the discontinuity of the conduction band, we face the well-known band-gap problem in the local-density approximation (LDA) calculations.[26] For binary semiconductors GaP and AlP, the indirect gaps at the X point are calculated to be 1.66 and 1.57 eV, respectively, compared with the corresponding measured values of 2.35 and 2.51 eV.[24] The band gap of the $(\mathrm{GaP})_4(\mathrm{AlP})_4$ superlattice is estimated to be 1.53 eV. By correcting the energy gap of the superlattice with a weighted average of the LDA gap errors of binary compounds, which is about 0.82 eV, we estimate the band gap of the (4×4) superlattice to be 2.35 eV. This value is in good agreement with the recent experimental result of photoluminescence measurements for the (4×4) GaP-AlP system.[9] Thus we assume that ΔE_v will not be affected significantly by including corrections to the LDA band gaps. With the use of the measured band gaps[24] and the calculated value for ΔE_v, the conduction-band discontinuity ΔE_c is determined as shown in Fig. 2. When AlP is grown on GaP substrate, the degenerate minimum conduction-band states X_{1c} of AlP are split by the substrate-induced tetragonal distortion. In this case, the energy of the $\Gamma(X_{1c})$ state, which is folded from the X_{1c} level, is higher by about 0.03 eV than the unfolded $M(X_{1c})$ state because the X_{1c} state decreases as the corresponding in-plane lattice constant decreases in epitaxial formation. A discontinuity of the conduction band is estimated to be 0.38 eV for the $\Gamma(X_{1c})$ state of AlP and 0.35 eV for the $M(X_{1c})$ state. Thus we conclude that the GaP-AlP system is a type-II superlattice, with the quantum wells for electrons in the AlP layers, in good agreement with recent experiments.[9]

C. Pseudodirect gap

Both GaP and AlP have six equivalent conduction-band minima at the X points in the zinc-blende structure. The zone-folding effect brings the X points lying in the superlattice growth direction (z direction) to the center of the superlattice BZ while it leaves the X points on the superlattice planes unchanged. Thus, if one considers only the zone-folding effect, there are five equivalent conduction-band minima in the superlattice: one at the Γ point and the others at the M points. The degeneracy between these points is lifted through the band-mixing effect resulting from charge transfers at interfaces. For thick superlattices, the Kronig-Penney model which assumes an abrupt change of material property at interfaces is quite satisfactory in describing the electronic structure.[27] However, in ultrathin superlattices, since the charge transfer occurring at the interface significantly affects the band structure, self-consistent microscopic calculations are required to represent the interface behavior. Zhang and his co-workers described the energy gap of the GaAs-AlAs superlattices well by incorporating the interfacial bonding effect within the Kronig-Penney model.[28] They estimated the interface effects on the Γ_{1c} and X_{1c} states by considering the quantity of charge transfer and predicted a direct gap in the GaAs-AlAs superlattices. Wei and co-workers found significant changes in the energy levels of the ultrathin ordered GaAs-AlAs superlattices due to symmetry-enforced level repulsion between different symmetry states of the constituents which fold into equal-symmetry states in the ordered superlattices.[2,3]

Figure 3 shows the variations of the conduction-band minimum states at the Γ and M points of the $(GaP)_m(AlP)_m$ system with m ranging from 1 to 6. The monolayer and bilayer superlattices are found to be indirect semiconductors, with the unfolded $M(X_{1c})$ state lower in energy than the folded $\Gamma(X_{1c})$ state. The $\Gamma(X_{1c})$ state energy decreases faster than the $M(X_{1c})$ state with increasing m. We find an indirect-to-direct band-gap transition for m close to 3. Thus the band gaps of superlattices with $m \geq 3$ become pseudodirect.

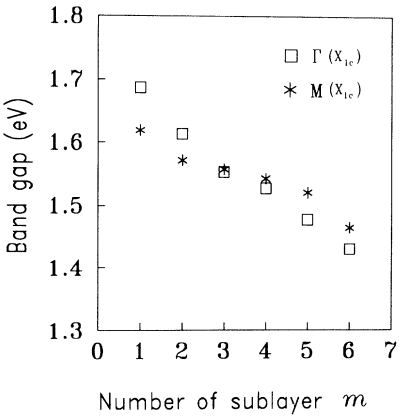

FIG. 3. Calculated energy gaps of the $(GaP)_m(AlP)_m$ superlattices where m ranges from 1 to 6 are plotted for the folded $\Gamma(X_{1c})$ and unfolded $M(X_{1c})$ states.

For the ultrathin superlattices with $m=1$ and 2, the band-mixing effect through the interfaces between the two constituents is dominant in forming the electronic structure of the indirect gap. Because of the difference between the cation potentials at interfaces, the electron charges are transferred from less ionic to more ionic atom for the bonding states, while for the antibonding states, i.e., the conduction bands, the direction of the charge transfer is reversed.[29] The folded $\Gamma(X_{1c})$ state is found to be composed of the anion p_z orbitals while the unfolded $M(X_{1c})$ points consist of the anion p_x or p_y orbitals. Since the charge transfer at interfaces occurs mainly along the superlattice direction, the $\Gamma(X_{1c})$ state is expected to be affected more significantly than the $M(X_{1c})$ state by the formation of superlattices. In fact, the charge transfer for the M state is found to be nearly neglected for the $m=1$ superlattice. Figure 4 shows the planar averaged charge densities for the conduction-band minimum states at the Γ and M points. In the monolayer superlattice, the electron charge densities associated with the $\Gamma(X_{1c})$ state are more accumulated in the Ga-P bonds, while the charge transfer for the M conduction-band state is not distinguishable. Since the GaP layers become quantum barriers in the GaP-AlP superlattices, the charge-transfer effect at interfaces puts the $\Gamma(X_{1c})$ state above the M state, resulting in an indirect-gap material. The interfacial bonding effect is also the main reason of the indirect band gap in the (2×2) superlattice because the charge confinement (this will be discussed later) is not significantly developed, as shown in Fig. 4.

To examine the mixing of the energy states of the con-

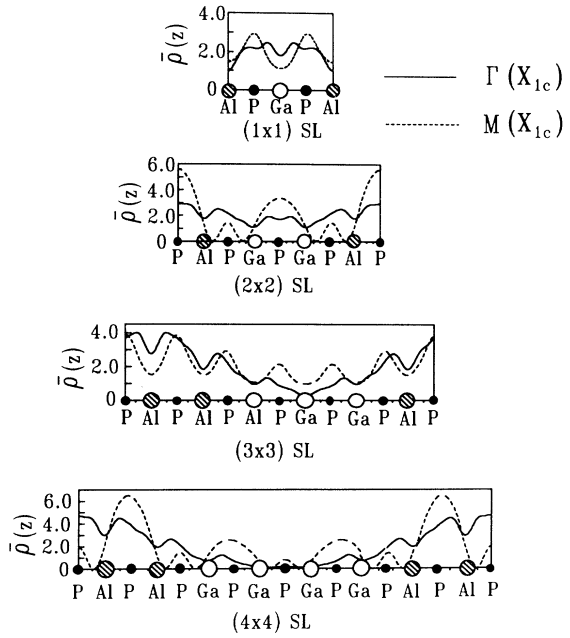

FIG. 4. Planar averaged charge densities of the GaP-AlP system are plotted along the superlattice (SL) direction for the folded $\Gamma(X_{1c})$ (solid line) and unfolded $M(X_{1c})$ (dotted line) states. The total charge density over the cell volume is set to be two electrons.

stituent materials in the $m=1$ and 2 superlattices, the energy shift due to the repulsion of distinct alloy states (α_1,k_1) and (α_2,k_2) which fold in the superlattices into states (λ_1,k) and (λ_2,k) of identical symmetry is calculated as follows:[2]

$$\Delta E^{(m)}_{\lambda_1,\lambda_2}=\frac{|\langle\psi_{\alpha_1,k_1}|\Delta V^{(m)}|\psi_{\alpha_2,k_2}\rangle|^2}{\epsilon_{\alpha_1,k_1}-\epsilon_{\alpha_2,k_2}}\ , \tag{2}$$

where $\psi_{\alpha,k}$ and $\epsilon_{\alpha,k}$ denote the eigenstate and the corresponding eigenvalue for an alloy. Here, $\Delta V^{(m)}$ is the difference between the potential of the $Ga_{0.5}Al_{0.5}P$ alloy and that of the $(GaP)_m(AlP)_m$ superlattice. We use virtual-crystal approximation to calculate the alloy potential, thus the energy levels of the alloy are independent of m. If the states $\psi_{\alpha_1,k}$ and $\psi_{\alpha_2,k}$ have the same symmetry at a wave vector k in the superlattice Brillouin zone, the matrix element in Eq. (2) is nonzero. Since the matrix element is also nonzero only if the relative phase of two repelling states is in phase with the potential difference ΔV^m, symmetry and relative phase are the major factors in determining the energy shift in level repulsion.[2]

The results of our calculations are given in Table II. We find that the alloy energy levels with the first- and second-order corrections of the perturbed potential given in Eq. (2) are in good agreement with the corresponding energies calculated directly for the superlattices. In the $m=1$ superlattice, the dominant repelling states at the center of the superlattice BZ are the folded $\Gamma(X_{1c})$ state and the valence-band maximum state Γ_{5v}. The energy shift in Eq. (2) is calculated to be about 0.05 eV for the $\Gamma(X_{1c})$ state, positioning this level in a higher-energy state while the Γ_{5v} level is lowered by approximately the same amount. Although the Γ_{4v} and Γ_{5v} states are degenerate in the alloy, the level shift is nearly negligible for the Γ_{4v} state because of the different symmetry. At the M point, a similar level repulsion exists between the $M(X_{1c})$ state folded from the zinc-blende (1,0,1) point to the superlattice (1,0,0) point and the unfolded $M(X_{4v})$ state because of the identical symmetry. Since the difference between the two repelling state energies at the M point is larger than that at the Γ point, the energy shift of the M conduction-band minimum state is found to be smaller by an order of magnitude than that for the $\Gamma(X_{1c})$ conduction-band state. Thus the (1×1) system becomes an indirect-gap superlattice.

In the (2×2) superlattice, the repelling levels in Eq. (2) are different from those of the (1×1) system because of the different symmetry. At the Γ point, a level repulsion occurs between the $\Gamma(X_{1c})$ state folded from the zinc-blende (0,0,1) X_{1c} state and the $\Gamma(\Delta_{1c})$ state from the zinc-blende $(0,0,\frac{1}{2})$ point while at the M point the unfolded $M(X_{1c})$ and folded $M(W_{1c})$ states repel each other. Since the $\Gamma(\Delta_{1c})$ and $M(W_{1c})$ states lie above the $\Gamma(X_{1c})$ and $M(X_{1c})$ states, level repulsion provides a downward shift for both the X-derived $\Gamma(X_{1c})$ and $M(X_{1c})$ states. The $\Gamma(X_{1c})$ state is found to have an additional downward shift of 0.005 eV, resulting from the band repulsion by the $\Gamma(\Delta_{3c})$ state. The analysis of angular momentum decompositions of the wave functions shows that the X_{1c} and W_{1c} states have s and d characters on the anion and p and d characters on the cation sublattice, whereas the Δ_{1c} state is less symmetric with all s, p, and d components on both the anion and cation sublattices. Thus the matrix element in Eq. (2) is much reduced for the repelling pair at the Γ point. This leads to the energy shift $\Delta E^{(2)}$ at the M point, which is two times larger compared to the corresponding value at the Γ point, although the energy separation of 2.90 eV between the $M(X_{1c})$ and $M(W_{1c})$ states is larger than the difference of 0.89 eV between the pair states at the Γ point. As a result of it, the (2×2) superlattice becomes indirect at the M state.

Next, we discuss the origin of the direct gaps occurring in superlattices with $m\geq3$. In ultrathin (1×1) and (2×2) superlattices, since the conduction states are delocalized extending over both the GaP and AlP sublattices, their energies lie near the well centers within the Kronig-Penney model.[27] Thus, the interfacial chemical

TABLE II. Comparisons of the energy levels for $Ga_{0.5}Al_{0.5}P$ alloy in virtual-crystal approximation (VCA) with those for the monolayer ($m=1$) and bilayer ($m=2$) superlattices. The first- ($\Delta E_{(1)}$) and second-order ($\Delta E_{(2)}$) corrections by the potential difference between alloy and superlattices are given. The Γ_{4v} state is taken as reference level to compare with the energies of the superlattices where intertomic positions are unrelaxed ($E^{\rm unrel}$) and fully relaxed ($E^{\rm rel}$).

m	States	$E^{\rm VCA}$	$\Delta E_{(1)}$	$\Delta E_{(2)}$	$E^{\rm VCA}+\Delta E(1)$ $+\Delta E_{(2)}$	$E^{\rm unrel}$	$E^{\rm rel}$
1	Γ_{5v}	0.000	−0.005	−0.050	−0.049	−0.039	−0.048
	Γ_{4v}	0.000	−0.004	−0.002	0.000	0.000	0.000
	$M(X_{4v})$	−2.329	0.000	−0.003	−2.326	−2.338	−2.342
	$\Gamma(X_{1c})$	1.602	0.000	0.051	1.659	1.665	1.687
	$M(X_{1c})$	1.602	0.000	0.003	1.611	1.610	1.619
2	Γ_{5v}	0.000	−0.003	−0.016	−0.021	−0.015	−0.028
	Γ_{4v}	0.000	−0.002	0.004	0.000	0.000	0.000
	$\Gamma(\Delta_{1c})$	2.492	0.000	0.015	2.505	2.562	2.585
	$\Gamma(X_{1c})$	1.602	0.000	−0.020	1.580	1.584	1.613
	$M(X_{1c})$	1.602	0.000	−0.041	1.559	1.563	1.572
	$M(W_{1c})$	4.503	0.000	0.041	4.542	4.532	4.506

TABLE III. Calculated effective masses (in units of electron mass) along the [001] superlattice direction for the zinc-blende (0,0,1) and (1,0,0) X_{1c} states are given for binary GaP and AlP. Numbers in parentheses are experimental data from Ref. 24.

	AlP	GaP
$\Gamma[X_{1c}^{(001)}]$	0.92(2.2)	1.25(1.37)
$M[X_{1c}^{(100)}]$	0.26(0.25)	0.25(0.25)

shift is the major factor of determining direct or indirect gap, as discussed before. As shown in Fig. 4, the electron densities associated with the Γ and M superlattice conduction-band states tend to be accumulated in the AlP quantum wells as the lattice period increases. Such charge confinement occurs more significantly for the Γ state. This results from the difference between the effective masses at the equivalent zinc-blende X points. The calculated effective masses for both bulk AlP and GaP are given in Table III. The effective masses calculated along the [001] superlattice direction for the zinc-blende (0,0,1) X_{1c} state are found to be three to five times larger than those calculated for the (1,0,0) X_{1c} state. Thus, the Γ-associated electron with a large effective mass is localized preferentially on the AlP sublattice according to the Kronig-Penney model.[27] Thus the superlattice Γ state has an energy closer to well edge, compared with the unfolded M states, resulting in direct-gap superlattices. We note that this behavior becomes significant as the lattice period m increases.

D. Substrate strain effect

On GaP or AlP substrate, the strain induced by lattice mismatch is extremely small in GaP-AlP superlattices. The ultrathin (1×1) and (2×2) superlattices are found to be indirect on GaP and AlP substrates. However, these indirect-gap superlattices can be direct on substrates with large substrate lattice constants (a_s). Figure 5 shows the variations of the $\Gamma(X_{1c})$ and $M(X_{1c})$ conduction-band states on various substrates such as GaP, AlP, Si, and GaAs. The monolayer and bilayer superlattices are found to be direct for substrate lattice constants above 5.48 and 5.47 Å, respectively. In superlattices, the lattice constant parallel to substrate is restricted to be equal to that of a chosen substrate, while the lattice constant ($a_\perp$) perpendicular to the substrate is determined by minimizing the total energy. We find $a_\perp$ to decrease as a_s increases. Since in zinc-blende materials the minimum conduction-band energy at the X point normally increases with the decreasing of lattice constant, the X-derived Γ state along the superlattice direction has decreasing behavior when a_s increases in superlattices, while the M states derived from the on-plane X points have opposite behavior. Therefore, an indirect-to-direct transition is likely to occur as shown in Fig. 5, if substrates having large lattice constants are used. However, it should be noted that although a large substrate lattice constant is necessary to make the superlattice band gap direct, it may lead to the lattice instability because of the large strain introduced during growth.

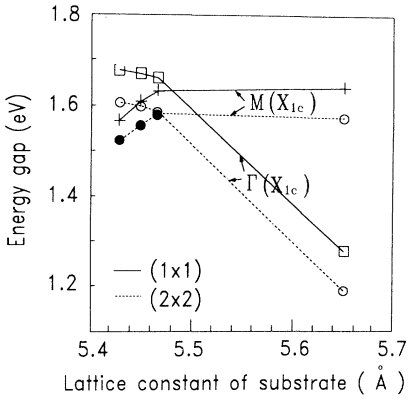

FIG. 5. Energy variations of the folded $\Gamma(X_{1c})$ and unfolded $M(X_{1c})$ states are plotted as a function of substrate lattice constant for the $(GaP)_m(AlP)_m$ superlattices with $m=1$ (solid) and 2 (dotted).

E. Optical transition

We examine the optical properties of superlattices by calculating the oscillator strength:[30]

$$f=\frac{2}{m_e\Delta E}|\langle\psi_c|p|\psi_v\rangle|^2 , \tag{3}$$

where ΔE is the gap energy between the conduction-band (ψ_c) and valence-band state (ψ_v), m_e is the free-electron mass, and p is the momentum operator. As shown in Fig. 6, the oscillator strength for the optical transition from the valence-band maximum state to the X_{1c}-derived conduction-band minimum state at the Γ point is nearly zero for superlattices with odd numbers of lattice period. In this case, the X_{3c}-derived state, which lies above the X_{1c}-derived state, has significantly larger oscillator strength. This oscillator strength tends to decrease with the increasing number of m. On the contrary, for superlattices with even numbers of m, the transition to the X_{1c}-derived conduction-band minimum state at the Γ point is optically allowed with large oscillator strength, while the X_3-derived Γ state has negligible strength.

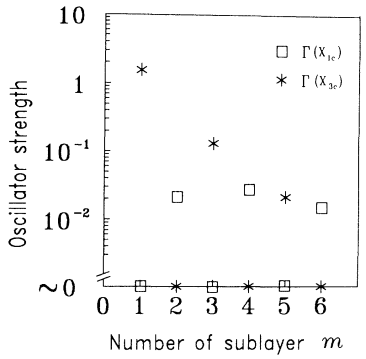

FIG. 6. The oscillator strengths for the transition from the valence-band maximum state to the X_{1c}- and X_{3c}-derived Γ states are plotted as a function of superlattice period m.

Our finding that oscillator strength is generally larger for shorter-period superlattices agrees well with recent photoluminescence measurements;[9] the emission intensity was found to increase with decreasing m where m ranges from 6 to 10 while the exceptionally small intensity observed for the $m=4$ superlattice was attributed to the inferior interface abruptness. Our results also agree fairly well with the tight-binding calculations by Kumagai, Takagahara, and Hanamura.[7] However, in their work, the calculations of the matrix elements for the $\Gamma(X_{3c})$ state were not made. Furthermore, since in this method the excited state s^* added to the conventional sp^3 orbits to describe the correct conduction band is s-like, the wave function as well as the oscillator strength for the folded $\Gamma(X_{1c})$ state with more d-like character may not be described properly.

IV. SUMMARY

Using the *ab initio* pseudopotential method, we have found that both the bulk and epitaxial GaP-AlP superlattices in the CuPt, CuAu-I, and chalcopyrite structures are structurally unstable at $T=0$. The GaP-AlP system is found to form the superlattices of a type-II band alignment and is a pseudodirect-gap semiconductor for superlattice periods $m \geq 3$, while it is indirect for $m=1$ and 2. As superlattice period increases, the charge confinements into the AlP quantum wells are more significant, resulting in the direct band gap. We have found that even the monolayer and bilayer superlattices, which are indirect on GaP substrate, can be direct if substrates with substrate lattice constants larger than 5.48 Å are used. The oscillator strength for the transition from the valence-band maximum to the conduction-band minimum state at the center of the superlattice Brillouin zone is found to be stronger for superlattices with even numbers of m and tends to decrease as m increases.

ACKNOWLEDGMENT

This work was supported in part by the Korean Science and Engineering Foundation.

[1]U. Gnutzmann and K. Clausecker, Appl. Phys. **3**, 9 (1974).
[2]S.-H. Wei and A. Zunger, Phys. Rev. B **39**, 3279 (1989); D. M. Wood, S.-H. Wei, and A. Zunger, *ibid.* **37**, 1342 (1988).
[3]S.-H. Wei and A. Zunger, J. Appl. Phys. **63**, 5794 (1988).
[4]D. L. Smith and C. Mailhiot, Rev. Mod. Phys. **62**, 173 (1990).
[5]For examples, see S. Satpathy, R. R. Martin, C. G. Van de Walle, I. Morrison, and M. Jaros, Phys. Rev. B **37**, 916 (1988); R. People and S. A. Jackson, *ibid.* **36**, 1310 (1987); U. Schmid, N. E. Christensen, and M. Cardona, *ibid.* **41**, 5919 (1990).
[6]J. Y. Kim and A. Madhukar, J. Vac. Sci. Technol. **21**, 528 (1982).
[7]M. Kumagai, T. Takagahara, and E. Hanamura, Phys. Rev. B **37**, 898 (1988).
[8]M. F. H. Schuurmans, H. W. A. M. Rompa, and R. Eppenga, J. Lumin. **37**, 269 (1987).
[9]A. Morii, I. Ohno, A. Kanda, K. Arai, K. Tokudome, K. Hara, J. Yoshino, and H. Kukimoto, Jpn. J. Appl. Phys. **30**, L1244 (1991).
[10]M. L. Cohen, Phys. Scr. **T1**, 5 (1982); J. Ihm, A. Zunger, and M. L. Cohen, J. Phys. C **12**, 4409 (1979).
[11]A. A. Mbaye, D. M. Wood, and A. Zunger, Phys. Rev. B **37**, 3008 (1988); J. E. Bernard, L. G. Ferreira, S.-H. Wei, and A. Zunger, *ibid.* **38**, 6338 (1988).
[12]P. Hohenberg and W. Kohn, Phys. Rev. **136**, B864 (1964); W. Kohn and L. J. Sham, *ibid.* **140**, A1133 (1965).
[13]D. M. Ceperly and B. J. Alder, Phys. Rev. Lett. **45**, 566 (1980); J. P. Perdew and A. Zunger, Phys. Rev. B **23**, 5048 (1981).
[14]D. R. Hamann, M. Schlüter, and C. Chiang, Phys. Rev. Lett. **43**, 1494 (1979).
[15]G. B. Bachelet and M. Schlüter, Phys. Rev. B **25**, 2103 (1982); L. Kleinman, *ibid.* **21**, 2630 (1980).
[16]S. Froyen, Phys. Rev. B **39**, 3168 (1989).
[17]D. J. Chadi and M. L. Cohen, Phys. Rev. B **8**, 5747 (1973).
[18]H. Hellmann, *Einführung in dir Quanten Theorie* (Deuticke, Leipzig, 1937), p. 285; R. P. Feynman, Phys. Rev. **56**, 340 (1939).
[19]P. N. Keating, Phys. Rev. **145**, 637 (1966); R. M. Martin, Phys. Rev. B **1**, 4005 (1970); J. L. Martins and A. Zunger, *ibid.* **30**, 6217 (1984).
[20]G. P. Srivastava, J. L. Martins, and A. Zunger, Phys. Rev. B **31**, 2561 (1985); **38**, 12 694 (1988).
[21]C. H. Park and K. J. Chang, Phys. Rev. B **45**, 11 755 (1992).
[22]P. Boguslawsk and A. Baldereschi, Phys. Rev. B **39**, 8055 (1989).
[23]C. G. Van de Walle and R. M. Martin, Phys. Rev. B **35**, 8154 (1987).
[24]*Landolt-Börnstein Tables,* edited by O. Madelung, M. Schulz, and H. Weiss, Landolt-Börnstein, New Series, Vol. 17a (Springer, Berlin, 1982), and references therein.
[25]J. Tersoff, J. Vac. Sci. Technol. B **4**, 1066 (1986).
[26]M. S. Hybertsen and S. G. Louie, Phys. Rev. Lett. **55**, 1418 (1985).
[27]H.-S. Cho and P. R. Prucnal, Phys. Rev. B **36**, 3237 (1987).
[28]S. B. Zhang, M. L. Cohen, and S. G. Louie, Phys. Rev. B **43**, 9951 (1991).
[29]J. C. Phillips, *Bonds and Bands in Semiconductors* (Academic, New York, 1973), p. 38.
[30]C. Cohen-Tannoudji, B. Diu, and F. Laloë, *Quantum Mechanics* (Hermann, Paris, 1977), Vol. 1, p. 1318.